OPEN

Proteomic Analysis of Transbronchial Biopsies to Discover Novel Biomarkers for Early Identification of Chronic Lung Allograft Dysfunction

Eisa Tahmasbpour, PhD,[1] Ashleigh Philp, PhD,[2,3] Vanathi Sivasubramaniam, MD[2,4] Claire Thomson, MD[1,5] Marshall Plit, MD, PhD,[1,6] Anjaneyaswamy Ravipati, PhD,[7] Mark Raftery, PhD,[7] and David Darley, MD, PhD[1,6]

Background. Chronic lung allograft dysfunction (CLAD) is a major contributor to poor long-term survival after lung transplantation (LTx). There is a paucity of validated tissue biomarkers which limits the early detection of CLAD. The aim of this study was to discover novel tissue proteins in CLAD. **Methods.** A longitudinal cohort study analyzed 15 tissue specimens from 2 groups of bilateral LTx recipients; those with CLAD (n = 3) and those without CLAD (n = 3). In both groups, transbronchial biopsies (TBBx) were retrieved from 2 timepoints; stable surveillance at 90 d after transplant, and during episodes of acute lung allograft dysfunction. In the CLAD cohort, additional tissue from explant CLAD lungs collected at retransplantation was analyzed. Proteomics analysis and immunohistochemistry were used to identify and validate differentially expressed proteins. **Results.** Tissue upregulation of a number of proteins including SerpinB1, SerpinH1, Cofilin 1, MUC1, COL15A1, COL4A4, and Coronin1B was found in recipients with CLAD. This finding was present when comparing CLAD onset and explant pathology to stable surveillance among recipients with CLAD and evident when compared with recipients without CLAD. Most of the upregulated tissue proteins in patients with CLAD had collectively critical roles in leukocytes migration and activation, inflammation, free radicals production and oxidative stress, epithelial–mesenchymal transition, myofibroblasts activation, and excessive deposition of extracellular matrix, which in turn enhance the risk of lung fibrosis and graft rejection. We also found exclusive expression of HLA-DQB1, JCHAIN, SAP18, FUCA1, MZB1, G3BP2, and BTF3 in CLAD cases, indicating they could be specific biomarkers of CLAD. **Conclusions.** This study identifies distinct proteomes that are linked to CLAD development and consequently may be a useful indicator for identifying LTx patients at higher risk of CLAD.

(*Transplantation Direct* 2025;11: e1800; doi: 10.1097/TXD.0000000000001800.)

Lung transplantation (LTx) is offered to select patients with advanced lung disease to improve their survival and quality of life. Graft survival after LTx is the shortest of all solid-organ transplants.[1] Chronic lung allograft dysfunction (CLAD), which develops in half of recipients by 5 y, is the most common cause of graft failure and poor survival after lung transplantation.[2,3] CLAD is characterized by allograft inflammation and fibrosis with 2 main phenotypes, restrictive allograft syndrome and bronchiolitis obliterans syndrome.[2] Currently, there are no diagnostic biomarkers routinely used to identify patients at higher risk of CLAD post-LTx. The diagnosis of CLAD is based on spirometric, volumetric, and

Received 23 December 2024. Revision received 24 February 2025.

Accepted 12 March 2025.

[1] Department of Thoracic Medicine and Lung Transplantation, St Vincent's Hospital Sydney, University of New South Wales, Sydney, NSW, Australia.

[2] School of Clinical Medicine, UNSW Medicine and Health, St Vincent's Healthcare Clinical Campus, University of New South Wales, Sydney, Australia.

[3] Centre for Inflammation, Centenary Institute, and Faculty of Science, University of Technology Sydney, Camperdown, NSW, Australia.

[4] Department of Anatomical Pathology, St Vincent's Hospital Darlinghurst, Sydney, NSW, Australia.

[5] Hunter Medical Research Institute, University of Newcastle Medical Sciences, Newcastle, NSW, Australia.

[6] St Vincent's Clinical Campus, Faculty of Medicine and Health, University of New South Wales, Sydney, NSW, Australia.

[7] Bioanalytical Mass Spectrometry Facility, University of New South Wales, Sydney, NSW, Australia.

This work was supported by a grant provided from the Alexandra and Loyd Martin Family Foundation, Australia. Eisa Tahmasbpour received The Carina Martin Lung Transplant Research Fellowship Award. This work was also supported by a grant provided by The Graham Painton Foundation, received by Ashleigh Philp.

The authors declare no conflicts of interest.

D.D. and M.P. designed this study. E.T. and A.P. performed experiments and analyzed data. T.C., A.R., M.R., V.S., and C.T. assisted with experiments and analysis of data. E.T. and D.D. wrote the article and revised the article. All authors commented on the article.

Supplemental digital content (SDC) is available for this article. Direct URL citations appear in the printed text, and links to the digital files are provided in the HTML text of this article on the journal's Web site (www.transplantationdirect.com).

Correspondence: David Darley, MD, PhD, Darlinghurst, Sydney, NSW 2010, Australia. (david.darley@svha.org.au).

ISSN: 2373-8731

DOI: 10.1097/TXD.0000000000001800

radiologic criteria. Histopathologic examination of transbronchial biopsy (TBBx) performed at set timepoints early after lung transplant for routine surveillance and for acute drops in graft function thereafter, are conducted to identify acute cellular rejection, an established risk factor for CLAD.[4] There are no effective treatments to restore graft function after the onset of CLAD. Hence, there is an urgent need to identify biomarkers with high sensitivity and specificity for CLAD diagnosis as well as for patients at increased risk of CLAD.[5]

A growing number of studies have been focused on finding valuable predictors such as donor-derived cell-free DNA in bronchoalveolar lavage fluid (BALF), biopsy and serum samples for early diagnosis of CLAD.[6,7] Although some biomarkers show promise in identifying CLAD, none are universally accepted for routine clinical practice because of their low specificity and their occurrence late in the disease process.[8-11] Furthermore, most of discovered biomarkers have been developed based on case-control study that might be less clinically effective. After CLAD onset, the disease behavior can vary. Some patients exhibit a slow decline in graft function over many years, with some progressing much more rapidly. By definition, CLAD is an irreversible state.[12] Validation of biomarkers for the early diagnosis of CLAD may allow for future interventions that prevent disease onset or slow progression of graft loss. With these challenges in mind, we aimed to use allograft tissue collected longitudinally after LTx to discover early protein biomarkers which may predict future CLAD. We hypothesize that novel proteins, upregulated along the pathologic trajectory towards CLAD may provide novel biomarker discovery, improve our mechanistic understanding and provide novel therapeutic targets for this condition.

MATERIALS AND METHODS

Patients and Samples Collection

We performed a single-center, longitudinal cohort study using biobanked lung transplant tissue from recipients who underwent a bilateral LTx from May 2012 to May 2018 at St. Vincent's Hospital (Sydney, Australia). The study procedure was reviewed and approved by the human ethics committee of St. Vincent's Hospital (Ethics number: 2020/ETH01356). A waiver of consent was obtained as all specimens were collected as part of routine clinical care. Both TBBx and CLAD explant tissue was biobanked in the form of formalin-fixed paraffin-embedded (FFPE) sample at the SydPath anatomical pathology department at St Vincent's Hospital, Sydney. Concurrent BALF for microbiology and cytology was collected at the same time as TBBx. Samples with positive microbiology test results were excluded from the study. We chose 15 biobanked TBBx tissues from 2 groups of bilateral LTx recipients who experienced acute lung allograft dysfunction (ALAD); those who developed CLAD (n = 3), diagnosed by International Society for Heart and Lung Transplantation 2019 Consensus criteria,[13] and those who did not develop CLAD (n = 3). In both groups, TBBx were retrieved from 2 timepoints: (1) stable surveillance at 90 d after transplant and (2) during the episode of ALAD. In the CLAD cohort, additional tissue from explant lungs was collected at the time of retransplantation. A consort flow diagram describing the TBBx collection and study procedure is depicted in Figure 1. All methods were carried out in accordance with relevant guidelines and regulations approved by the St. Vincent's Hospital. The presence of CLAD was confirmed by longitudinal spirometry as per the International Society for Heart and Lung Transplantation 2019 CLAD consensus and phenotype criteria.

Proteomics Study and Bioinformatics Analysis

For proteomics analysis, FFPE tissues were deparaffinated (**Supplemental Method 1, SDC**, http://links.lww.com/TXD/A759) and then proteins were extracted and digested (**Supplemental Method 2, SDC**, http://links.lww.com/TXD/A759) using Qproteome FFPE Tissue Kit (QIAGEN) according to the manufacturer's protocol. Peptides were then subjected to liquid-chromatography mass spectrometry (**Supplemental Method 3, SDC**, http://links.lww.com/TXD/A759). Differentially expressed proteins (DEPs) were identified and quantified using bioinformatic tools (**Supplemental Method 4, SDC**, http://links.lww.com/TXD/A759).

Immunohistochemistry Staining

A set of proteins of interest were selected to be validated by immunohistochemistry (IHC) staining (**Supplemental Method 5, SDC**, http://links.lww.com/TXD/A759).

Data Analysis

Quantitative clinical results are presented as median and interquartile range (IQR) and compared using the Mann-Whitney test. The percentages and frequencies of each item between groups were compared using Crosstabs and Chi-square tests. P values <0.05 were considered statistically significant. The SPSS software (IBM, version 22) was used to analyze the data.

RESULTS

Clinical Outcomes

The patient characteristics and information about the donors are presented in **Table S1** (**SDC**, http://links.lww.com/TXD/A759). The study included a total of 15 tissue specimens collected from 6 LTx recipients. The median (interquartile range) recipient age at transplant was 31 (22–62) y. All recipients underwent bilateral lung transplantation, 4 for cystic fibrosis, 1 idiopathic pulmonary fibrosis, and 1 Chronic obstructive pulmonary disease. The study cohort included n = 3 patients who were diagnosed with clinical CLAD with pathologic diagnosis confirmed on explant pathology at the time of retransplantation. The comparison cohort included n = 3 patients who underwent TBBx to investigate ALAD, with a resolution back to normal allograft function without CLAD. The median time from LTx to ALAD in CLAD and non-CLAD groups was 58 (41–58) and 12 (7–29) mo (P = 0.047), respectively. The median time from ALAD to CLAD was 8 (1–11) mo in CLAD group (**Table S1, SDC**, http://links.lww.com/TXD/A759).

Protein Identification and Quantification

A liquid-chromatography mass spectrometry analysis produced 128 378 spectra corresponding to 10 876 unique peptides representing 3323 proteins. The protein identification was considered accepted if they could be established at 99% protein threshold and 95% peptide threshold. Overall, 2362 quantifiable proteins were identified with the cutoff of $Q \leq 0.01$ using Mascot Percolator. A total of 2362 identified proteins contained >1 peptide, including 946 proteins with

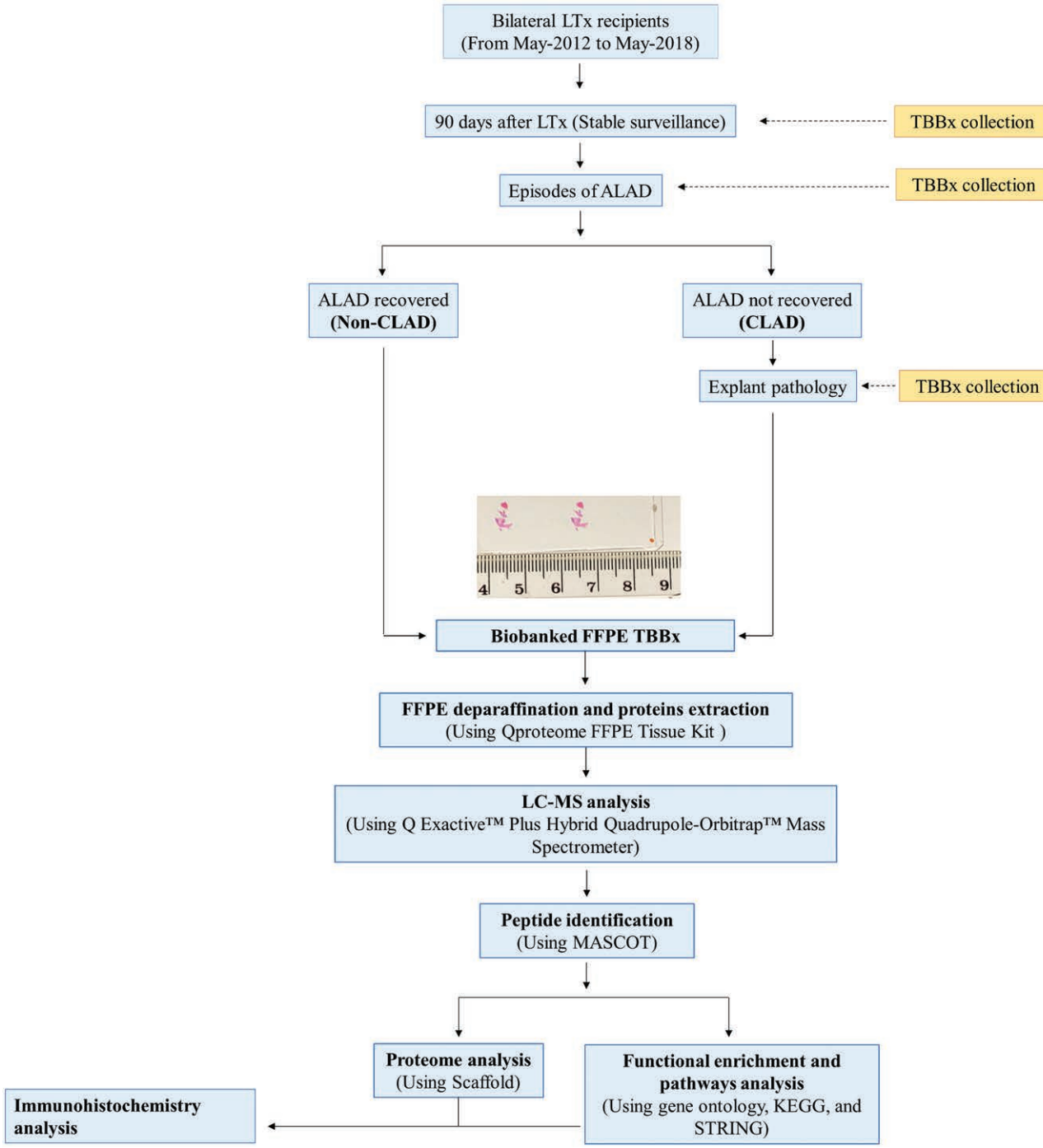

FIGURE 1. CONSORT diagram describing the study procedures (left side) and histopathologic features of TBBx in different groups (right side). TBBx sections of stable surveillance (A), CLAD onset (B), and explant pathology in patients who developed CLAD (C). TBBx sections of stable surveillance (D) and ALAD in patients without diagnosis of CLAD (E). All images taken at 40× magnification. ALAD, acute lung allograft dysfunction; CLAD, chronic lung allograft rejection; FFPE, formalin-fixed paraffin-embedded; KEGG, Kyoto Encyclopedia of Genes and Genomics; LC-MS, liquid-chromatography mass spectrometry; LTx, lung transplantation; TBBx, transbronchial biopsy.

≥5 peptides, 270 proteins with 4 peptides, 412 proteins with 3 peptides, and 734 proteins with 2 peptides. For sufficient stringency and confidence in proteomics data, we filtered to the proteins with ≥2 unique peptides. Comparisons were made in the DEPs comparing: (1) CLAD patients at the following time points: stable 3-mo surveillance, ALAD at the time of CLAD onset and explant tissue and (2) patients without CLAD at the following time points: stable 3-mo surveillance and ALAD with subsequent recovery to normal baseline allograft function.

Proteomics Analysis of Longitudinal Tissue Samples in Patients Diagnosed With CLAD

The proteomics data were analyzed by Scaffold Software, and then, the proteins homology and their expression pattern were shown in Venn diagrams and Volcano plots, respectively.

Among recipients with CLAD, the protein expression pattern showed that 862 (41.16%) proteins were common to all timepoints, whereas 92, 429, and 166 proteins were unique to TBBx in the stable surveillance, CLAD onset, and explant tissue groups, respectively (Figure 2A).

As shown in Venn diagram processed by Scaffold Software, there was low homology between proteins detected at CLAD onset compared with the surveillance timepoint at 50.1% (Figure 2B). With a cutoff of a > 1.5-fold change in expression and $P < 0.05$ processed by Scaffold Software, an average of 84 DEPs was identified in CLAD onset compared with stable surveillance, of which 81 ones were upregulated and 3 ones were downregulated. SND1, SEPTIN9, Rpl7a, RPL30, ACAA2, RUVBL2, TST, AKAP2, CAPZA2, Mapk1, RPL5, and CORO1B were the most upregulated proteins (Table 1). Volcano plot confirmed a significant difference in protein

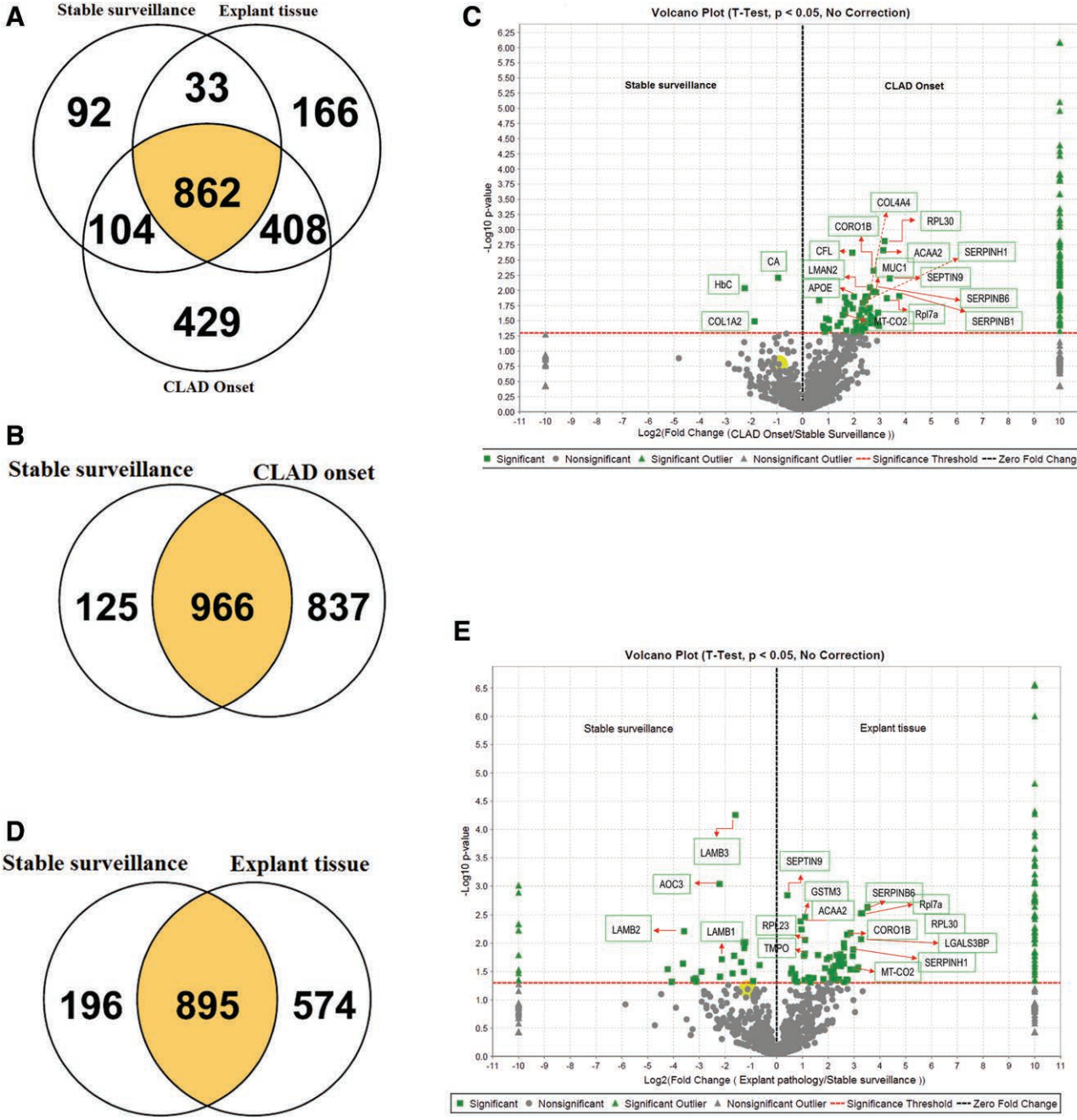

FIGURE 2. Proteomic homology and Volcano plot of DEPs in CLAD patients. A, Venn diagram showing the overlap of expressed proteins between all groups. A total of 862 (41.16%) proteins were found to be expressed in all 3 groups. The protein homology between stable surveillance with CLAD onset (B) and explant pathology was 50.1% (966 shared proteins) (D) and 53.75% (895 shared proteins), respectively. Volcano plot of DEPs between stable surveillance and CLAD onset (C), stable surveillance and explant pathology (E). Volcano plot depicts the log2 fold change (x-axis) vs -log10 *Q* value (y-axis, representing the probability that the protein is differentially expressed). $P < 0.05$ and fold change ≥1.25 were set as the significant threshold (red line) for differential expression. Dots in green denote significantly upregulated proteins which passed the screening threshold. Black dots present non-significantly DEPs. CLAD, chronic lung allograft rejection; DEPs, differentially expressed proteins.

TABLE 1.

Top 60 upregulated proteins in CLAD onset TBBx compared with surveillance TBBx in CLAD patients

Protein	Description	Fold change	*P*
SND1	Staphylococcal nuclease domain-containing protein 1	14	0.012
SEPTIN9	Septin-9	10	0.006
Rpl7a	60S ribosomal protein L7a	9.7	0.013
RPL30	60S ribosomal protein L30	9.1	0.001
ACAA2	3-ketoacyl-CoA thiolase, mitochondrial	8.8	0.002
RUVBL2	RuvB-like 2	7.8	0.038
TST	Thiosulfate sulfurtransferase	7.6	0.023
AKAP2	A-kinase anchor protein 2	7.4	0.036
CAPZA2	F-actin-capping protein subunit alpha-2	7.2	0.011
Mapk1	Mitogen-activated protein kinase 1	6.9	0.029
RPL5	60S ribosomal protein L5	6.9	0.033
CORO1B	Coronin-1B	6.8	0.004
SERPINB6	Serpin B6	6.8	0.011
RALA	Ras-related protein Ral-A	6.7	0.010
HNRNPUL2	Heterogeneous nuclear ribonucleoprotein U-like protein 2	6.3	0.030
PDHB	Pyruvate dehydrogenase E1 component subunit beta, mitochondrial	6.3	0.030
LMAN2	Vesicular integral-membrane protein VIP36	6.2	0.008
TMPO	Lamina-associated polypeptide 2, isoforms beta/gamma	6.2	0.027
DERA	Deoxyribose-phosphate aldolase	6.2	0.035
NDUFA13	NADH dehydrogenase [ubiquinone] 1 alpha subcomplex subunit 13	6.1	0.019
HNRNPA0	Heterogeneous nuclear ribonucleoprotein A0	5.9	0.023
G6PD	Glucose-6-phosphate 1-dehydrogenase	5.8	0.013
EIF4H	Eukaryotic translation initiation factor 4H	5.8	0.023
RPL23	60S ribosomal protein L23	5.5	0.013
SARG	Specifically androgen-regulated gene protein	5.4	0.015
LGALS3BP	Galectin-3-binding protein	5.4	0.042
HNRNPH2	Heterogeneous nuclear ribonucleoprotein H2	5.3	0.033
RPS17	40S ribosomal protein S17	5.2	0.021
METTL7A	Methyltransferase-like protein 7A	5.2	0.032
VAPA	Vesicle-associated membrane protein-associated protein A	5.1	0.016
TXN	Thioredoxin	5	0.039
LCN2	Neutrophil gelatinase-associated lipocalin	4.9	0.021
CNN3	Calponin-3	4.9	0.029
ATIC	Bifunctional purine biosynthesis protein ATIC	4.9	0.047
GSTM3	Glutathione S-transferase Mu 3	4.7	0.030
POR	NADPH--cytochrome P450 reductase	4.6	0.026
STAT3	Signal transducer and activator of transcription 3	4.6	0.026
COL4A4	Collagen alpha-4(IV) chain	4.6	0.038
RPS15	40S ribosomal protein S15	4.5	0.039
ACP1	Low molecular weight phosphotyrosine protein phosphatase	4.2	0.033
TRA2B	Transformer-2 protein homolog beta	4.2	0.043
UQCRFS1	Cytochrome b-c1 complex subunit Rieske, mitochondrial	4.1	0.047
MGP	Matrix Gla protein	4.1	0.047
APOE	Apolipoprotein E	4	0.013
PABPC1	Polyadenylate-binding protein 1	3.9	0.020
DLST	Dihydrolipoyllysine-residue succinyltransferase	3.9	0.048
LRP1	Prolow-density lipoprotein receptor-related protein 1	3.8	0.002
Sec22b	Vesicle-trafficking protein SEC22b	3.6	0.017
SERPINH1	Serpin H1	3.6	0.029
MUC1	Mucin-1	3.5	0.041
VDAC1	Voltage-dependent anion-selective channel protein 1	3.4	0.017
GNAQ	Guanine nucleotide-binding protein G(q) subunit alpha	3.3	0.016
KHSRP	Far upstream element-binding protein 2	3.3	0.046
COL15A1	Collagen alpha-1(XV) chain	3.2	0.014
PML	Protein PML	3.1	0.013
ATP6V1A	V-type proton ATPase catalytic subunit A	3.1	0.021
VPS35	Vacuolar protein sorting-associated protein 35	3.1	0.024
IDH2	Isocitrate dehydrogenase [NADP], mitochondrial	2.9	0.025
MT-CO2	Cytochrome c oxidase subunit 2	2.9	0.034
RPL19	60S ribosomal protein L19	2.8	0.034

CLAD, chronic lung allograft rejection; TBBx, transbronchial biopsy.

TABLE 2.

Top 60 upregulated proteins in explant TBBx compared with surveillance TBBx in CLAD patients

Protein	Description	Fold change	*P*
ACAA2	3-ketoacyl-CoA thiolase, mitochondrial	11	0.002
EIF4B	Eukaryotic translation initiation factor 4B	10	0.003
ATP6V1B2	V-type proton ATPase subunit B, brain isoform	9.7	0.008
Rpl7a	60S ribosomal protein L7a	9.6	0.003
SEPTIN9	Septin-9	8.9	0.027
FASN	Fatty acid synthase	8.6	0.029
POR	NADPH–cytochrome P450 reductase	7.9	0.010
VARS1	Valine–tRNA ligase	7.8	0.013
GSTM3	Glutathione S-transferase Mu 3	7.7	0.017
NDUFA13	NADH dehydrogenase	7.3	0.029
RPL30	60S ribosomal protein L30	7.2	0.006
PA2G4	Proliferation-associated protein 2G4	6.7	0.006
SARG	Specifically androgen-regulated gene protein	6.7	0.007
LPCAT1	Lysophosphatidylcholine acyltransferase 1	6.7	0.045
IGLC2	Immunoglobulin lambda constant 2 O	6.5	0.044
HDGF	Hepatoma-derived growth factor	6.1	0.010
TMPO	Lamina-associated polypeptide 2, isoforms beta/gamma	6.1	0.012
COPG1	Coatomer subunit gamma-1	6.1	0.023
ACOT2	Acyl-coenzyme A thioesterase 2, mitochondrial	6.1	0.049
HNRNPA0	Heterogeneous nuclear ribonucleoprotein A0	6.0	0.017
RPL23	60S ribosomal protein L23	5.7	0.020
Mapk1	Mitogen-activated protein kinase 1	5.6	0.021
PYCARD	Apoptosis-associated speck-like protein containing a CARD	5.6	0.025
UQCRFS1	Cytochrome b-c1 complex subunit Rieske, mitochondrial	5.6	0.029
HEBP1	Heme-binding protein 1	5.5	0.016
OXSR1	Serine/threonine-protein kinase OSR1	5.5	0.016
LGALS3BP	Galectin-3-binding protein	5.3	0.020
PSMA4	Proteasome subunit alpha type-4	5.3	0.043
BLVRA	Biliverdin reductase A	5.2	0.013
RPS15	40S ribosomal protein S15	5.0	0.016
NAPRT	Nicotinate phosphoribosyltransferase	5.0	0.044
CORO1B	Coronin-1B	4.9	0.013
ARHGDIB	ρ GDP-dissociation inhibitor 2	4.8	0.025
FBP1	Fructose-1,6-bisphosphatase 1	4.7	0.038
ERP44	Endoplasmic reticulum resident protein 44	4.6	0.027
ARHGDIA	ρ GDP-dissociation inhibitor 1	4.6	0.027
DLST	Dihydrolipoyllysine-residue succinyltransferase	4.6	0.030
DERA	Deoxyribose-phosphate aldolase	4.6	0.044
AK2	Adenylate kinase 2, mitochondrial	4.5	0.010
MAPK3	Mitogen-activated protein kinase 3	4.5	0.025
CAPZA1	F-actin-capping protein subunit alpha-1	4.5	0.039
PRPS1	Ribose-phosphate pyrophosphokinase 1	4.4	0.031
TXN	Thioredoxin	4.4	0.037
KNG1	Kininogen-1	4.4	0.042
G6PD	Glucose-6-phosphate 1-dehydrogenase	4.4	0.049
RPL24	60S ribosomal protein L24	4.2	0.032
SERPINB6	Serpin B6	4.2	0.041
TYMP	Thymidine phosphorylase	4.1	0.018
PSME2	Proteasome activator complex subunit 2	4.1	0.025
MT-CO2	Cytochrome c oxidase subunit 2	3.9	0.013
PSMB10	Proteasome subunit beta type-10	3.9	0.015
EEF2	Elongation factor 2	3.9	0.019
ARPC1B	Actin-related protein 2/3 complex subunit 1B	3.8	0.041
APRT	Adenine phosphoribosyltransferase	3.7	0.028
EDF1	Endothelial differentiation-related factor 1	3.5	0.034
SFTPA2	Pulmonary surfactant-associated protein A2	3.5	0.043
CCT7	T-complex protein 1 subunit eta	3.5	0.044
PRDX2	Peroxiredoxin-2	3.2	0.032
CCT2	T-complex protein 1 subunit beta	3.0	0.014
SERPINH1	Serpin H1	3.0	0.014

CLAD, chronic lung allograft rejection; TBBx, transbronchial biopsy.

expression pattern between CLAD onset and stable surveillance tissue (Figure 2C).

Venn diagram analysis in Scaffold Software revealed a low protein homology between stable surveillance TBBx and explant tissue at 53.75% (Figure 2D). A total of 126 DEPs (including 96 upregulated proteins and 30 downregulated proteins) were found in explant tissue compared with stable surveillance state. ACAA2, EIF4B, ATP6V1B2, Rpl7a, SEPTIN9, FASN, POR, VARS1, GSTM3, and NDUFA13 were the top 10 most upregulated proteins (Table 2). Volcano plot revealed a significant difference in expression pattern of DEPs between explant and stable surveillance TBBx (Figure 2E).

We applied gene ontology (GO) enrichment analysis to reveal the biological roles of DEPs and function of DEPs in CLAD tissue. The top 10 most enriched processes for upregulated proteins processed by GO enrichment analysis at CLAD onset are depicted in Figure 3. The most enriched biological processes were RNA catabolic process, translational inhibition, and interleukin (IL)-12-mediated signaling pathway (Figure 3A). We used chord plot to show the relationship between GO term and proteins. Interaction network analysis by chord plot identified 43 top proteins such as CFL-1, SND1, RPL5, and GSTO1 associated with these processes (**Figure S1A, SDC**, http://links.lww.com/TXD/A759). The most enriched cell components were: focal adhesion, cell-substrate junction, oxidoreductase complex, collagen-containing extracellular matrix, and respiratory chain complex (Figure 3B). We explored 30 top proteins such as SERPINA3, SERPINB1, SERPINC1, SERPINH1, COL4A4, SERPINB6, CFL-1, CORO1B, and CORO1C that were contributed to these cellular processes (**Figure S1B, SDC**, http://links.lww.com/TXD/A759). The most enriched molecular functions were cadherin binding, RNA binding, and antioxidant (Figure 3C). The network analysis discovered 37 top proteins such as CFL-1, SERPINB1, SERPINC1, SERPINH1, SERPINB6, CORO1C, SEPTIN9, and CORO1B that were involved in these molecular functions (**Figure S1C, SDC**, http://links.lww.com/TXD/A759).

The GO enrichment analysis was also performed for the uniquely expressed proteins (UEPs) to clarify their biological and molecular functions in CLAD TBBx. A total of 837 UEPs were identified in TBBx of patients at CLAD onset compared with their stable surveillance (**Table S2, SDC**, http://links.lww.com/TXD/A759). Neutrophil degranulation, neutrophil activation involved in immune response, antigen processing, and presentation, RNA catabolic process and electron transport chain were the most enriched biological processes at CLAD onset. The most enriched cellular compounds were mitochondrial matrix, mitochondrial protein complex, secretory granule lumen, cytoplasmic vesicle lumen, and respiratory chain complex. The most enriched molecular functions were: translation initiation factor activity, translation regulator activity, cadherin binding. List of all top proteins involved in these processes can be seen in **Figures S2A–C** (**SDC,** http://links.lww.com/TXD/A759).

The GO enrichment analysis was performed to explain the biological process and function of DEPs in explant tissue. The top 10 most enriched processes for upregulated proteins in explant tissue are depicted in Figure 4. The most enriched biological processes were: neutrophil degranulation, neutrophil activation involved in immune response, IL-12-mediated signaling pathways, response to IL-12, regulation of peptidases activity, and RNA catabolic process (Figure 4A). Interaction network analysis identified 43 top proteins including SERPINH1, SERPINC1, SERPINB1, MIF, CCT2, STING1, and CFL-1, associated with these processes (**Figure S3A, SDC**, http://links.lww.com/TXD/A759). The most enriched cell components were secretory granule lumen, cytoplasmic vesicle lumen, focal adhesion, azurophil granule lumen, and collagen-containing extracellular matrix (Figure 4B). We discovered 39 top proteins such as COL15A1, SERPINC1, MIF, SERPINB1, CFL-1, CCT8, CCT2, CORO1B, and CORO1C that were involved in these cellular processes (**Figure S3B, SDC**, http://links.lww.com/TXD/A759). The most enriched molecular functions were peptidases activity and binding (Figure 4C). The network associated with catalytic activity and binding was connected by 34 top proteins such as CFL-1, CORO1C, CCT8, SERPINB1, SERPINC1, SERPINH1, SERPINB6, SEPTIN9, and CORO1B (**Figure S3C, SDC**, http://links.lww.com/TXD/A759).

The GO enrichment analysis was also performed for the UEPs in explant tissue. compared with stable surveillance, the proteome of explant TBBx showed 574 UEPs (**Table S3, SDC**, http://links.lww.com/TXD/A759). Electron transport chain, neutrophil degranulation, neutrophil activation, and respiratory electron transport chain were the most enriched biological processes in explant tissues. The most enriched cellular compounds were mitochondrial matrix, secretory granule lumen, cytoplasmic vesicle lumen, oxidoreductase complex, and respiratory chain complex. The most enriched molecular functions were electron transfer activity, NADH dehydrogenase activity, and oxidoreductase activities. WARS1, DDX3X, EPX, NDUFs, PSM families (PSMB6, PSMF1, PSME1, PSMD5, PSMD6, PSMB5, PSMC6, and PSMC4), and so on were among the top proteins involved in these processes (**Figure S4A–C, SDC**, http://links.lww.com/TXD/A759).

The proteome analysis coupled with bioinformatic tools revealed that tissue alpha-L-fucosidase (FUCA1), Immunoglobulin J chain (JCHAIN), HLA class II histocompatibility antigen, DQ beta 1 chain (HLA-DQB1), and Histone deacetylase complex subunit SAP18 (SAP18) were exclusively expressed in 100%, 100%, 66.67%, and 66.67% of ALAD patients with subsequent progression to CLAD, respectively. These proteins were not detected in TBBx of recovered ALAD patients; therefore, we hypothesise that these proteins may be valuable tissue biomarkers to predict the risk of ALAD progression to CLAD in LTx patients.

Proteomics Analysis of Longitudinal Tissue in Recipients Without CLAD

The proteomics data were also analyzed by Scaffold Software in LTx patients without CLAD. The proteins homology and their expression pattern were depicted in Venn diagrams and Volcano plots, respectively. In patients without a diagnosis of CLAD, there was high protein homology (71.07%) observed between ALAD and stable surveillance tissue (Figure 5A). A total 43 DEPs were discovered in TBBx of patients at the time of ALAD when compared with their stable surveillance tissue, of which 6 proteins were upregulated and 37 ones were downregulated (**Table S4, SDC**, http://links.lww.com/TXD/A759). LCN2, APEH, PRPS1, LDHB, TF, and KRT10 were the upregulated proteins, whereas PRPSAP1, GRHPR, TST, RAD23B, ADIRF, and so on were among the most downregulated proteins

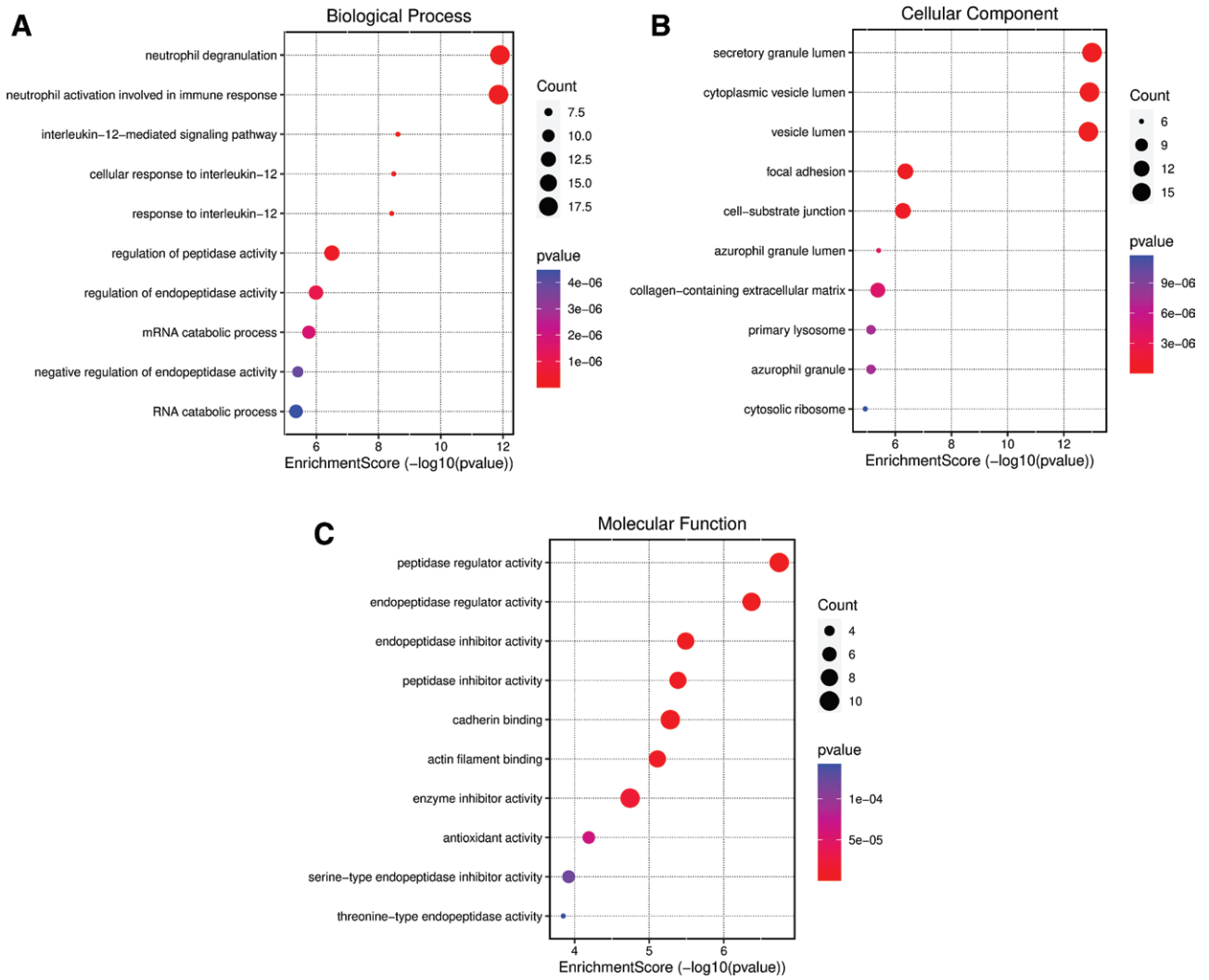

FIGURE 3. GO enrichment analysis of DEPs at the time point of CLAD onset compared with stable surveillance in patients with diagnosis of CLAD. The GO analysis for biological process (A), cellular component (B), and molecular function enriched by DEPs (C). The enrichment score is the ratio of the number of DEPs annotated to this pathway term to the total number of proteins annotated to this pathway term. A higher enrichment factor indicates greater intensiveness, a lower *P* value means greater intensiveness. The dot size represents the number of DEPs annotated to the pathway. CLAD, chronic lung allograft rejection; DEPs, differentially expressed proteins; GO, gene ontology.

(**Table S4, SDC,** http://links.lww.com/TXD/A759). Volcano plot revealed a mild difference in protein expression pattern between these groups (Figure 5B). GO enrichment analysis revealed that most of these DEPs contributed to different metabolic pathways.

Proteomics Analysis Comparing Diagnostic Tissue From Recipients With CLAD and Without CLAD

CLAD Onset Versus ALAD

There was moderate protein homology comparing CLAD patients to those without at the time of diagnostic biopsy to investigate ALAD at 67.53% (Figure 5C). A total of 74 DEPs (including 68 upregulated proteins and 6 downregulated proteins) were found in diagnostic TBBx in the CLAD recipients compared with those without. APOL2, QDPR, NAGK, SNRPA, SRP14, MAN2B1, COTL1, EIF3F, NECAP2, and PRPSAP1 were the top 10 most upregulated proteins at CLAD onset (Table 3). Volcano plots revealed a significant difference in expression pattern of DEPs between the 2 groups (Figure 5D). Protein targeting to membrane, protein targeting and localization to ER, neutrophil degranulation, neutrophil activation involved in immune response and oxidative phosphorylation were among the most enriched biological processes at CLAD onset. The most enriched cellular compounds were: cytosolic ribosome, focal adhesion, secretory granule lumen, and collagen-containing extracellular matrix. For the molecular function, DEPs were significantly involved in structural constituent of ribosome, rRNA binding, and endopeptidase regulator activity. SERPIN families, especially SERPINB1, SERPINF1, SERPINB9 and SERPINH1, were the most interesting proteins contributing to these pathways.

Stable Surveillance in CLAD Versus Non-CLAD Patients

There was mild proteome homology comparing TBBx surveillance between CLAD and non-CLAD patients (57.37%; Figure 5E). A total of 53 DEPs (including 48 upregulated proteins and 5 downregulated proteins) were found in TBBx

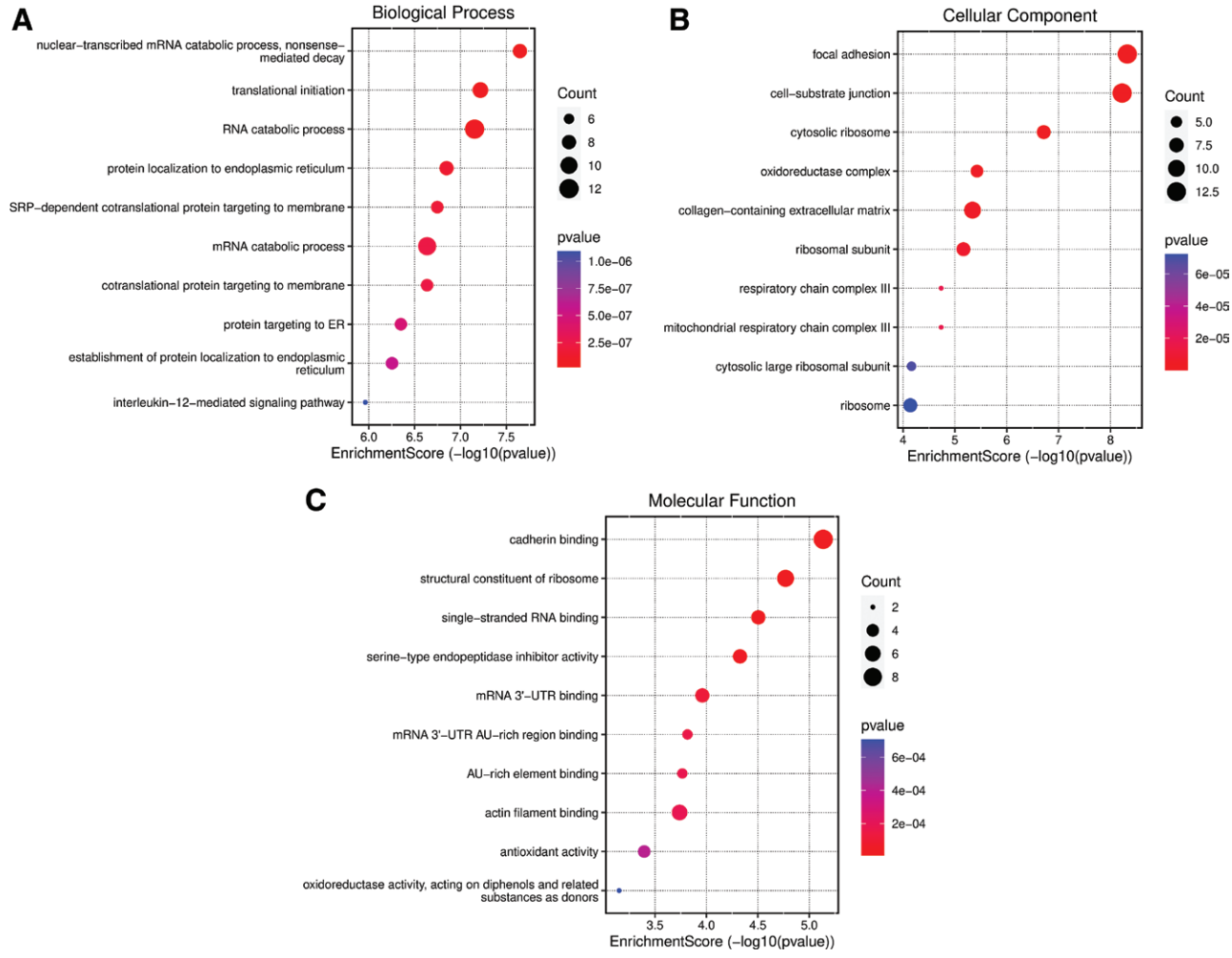

FIGURE 4. GO enrichment analysis of DEPs in explant tissues compared with stable surveillance in patients with diagnosis of CLAD. The GO analysis for biological processs (A), cellular component (B), and molecular function enriched by DEPs (C). The enrichment score is the ratio of the number of DEPs annotated to this pathway term to the total number of proteins annotated to this pathway term. A higher enrichment factor indicates greater intensiveness, a lower P-value means greater intensiveness. The dot size represents the number of DEPs annotated to the pathway. CLAD, chronic lung allograft rejection; DEPs, differentially expressed proteins; GO, gene ontology.

surveillance in the patients with CLAD compared with non-CLAD cases (Table 4). Volcano plots revealed a significant difference in protein expression pattern between the 2 groups (Figure 5F). Serpin B6, COL4A4, CORO1B, LGALS3BP, CCT7, and CCT8 were among the most interesting proteins that significantly upregulated in surveillance TBBx of patients with CLAD. A tendency toward upregulation of other proteins such as COL15A1 (2.8-fold), COL4A3 (2.1.-fold), COL15A1 (2.8-fold), MUC1 (2.9-fold), CFL-1 (1.7-fold), and SerpinH1 (3.7-fold) was found in CLAD cases; however, the *P* value was not significant.

Validation of Protein Expression Through IHC Analysis

Proteins of interest including SerpinB1, SerpinH1, Cofilin 1, and Coronin A were upregulated in explant and diagnostic allograft tissue in CLAD recipients compared with diagnostic tissue in those without CLAD. We performed IHC analysis of these proteins to validate the results of proteome data and presence of target proteins in tissue (Figure 6). Protein staining was observed in tissue of all groups with variations in staining intensity and pattern. Overall, staining intensity and expression pattern of Serpin B1 (Figure 6A), Coronin 1B (Figure 6B), Serpin H1, and Cofilin 1 (Figure 6C) were higher in CLAD patients compared with non-CLAD cases, representing the protein expression data are consistent with the proteomics data of the respective proteins.

DISCUSSION

To the best of our knowledge, this is the first longitudinal proteomic signature of lung grafts performed in different set points, from 3 mo post-LTx (stable grafts) to CLAD development and explant tissues. Our result, from a single-center longitudinal assessment of LTx recipients, identifies and validates the trajectory of number parenchymal tissue proteins which appear during the evolution of CLAD. Overall, we identified 2 groups of proteins that have the potential to be considered further for early diagnosis of CLAD. The first group of proteins were those that significantly upregulated in TBBx of CLAD when compared with the trajectory of tissue proteins identified in patients without CLAD. Proteins such as SerpinB1, SerpinH1, Cofilin 1, MUC1, COL15A1, COL4A4 and Coronin1B were included in this group. The

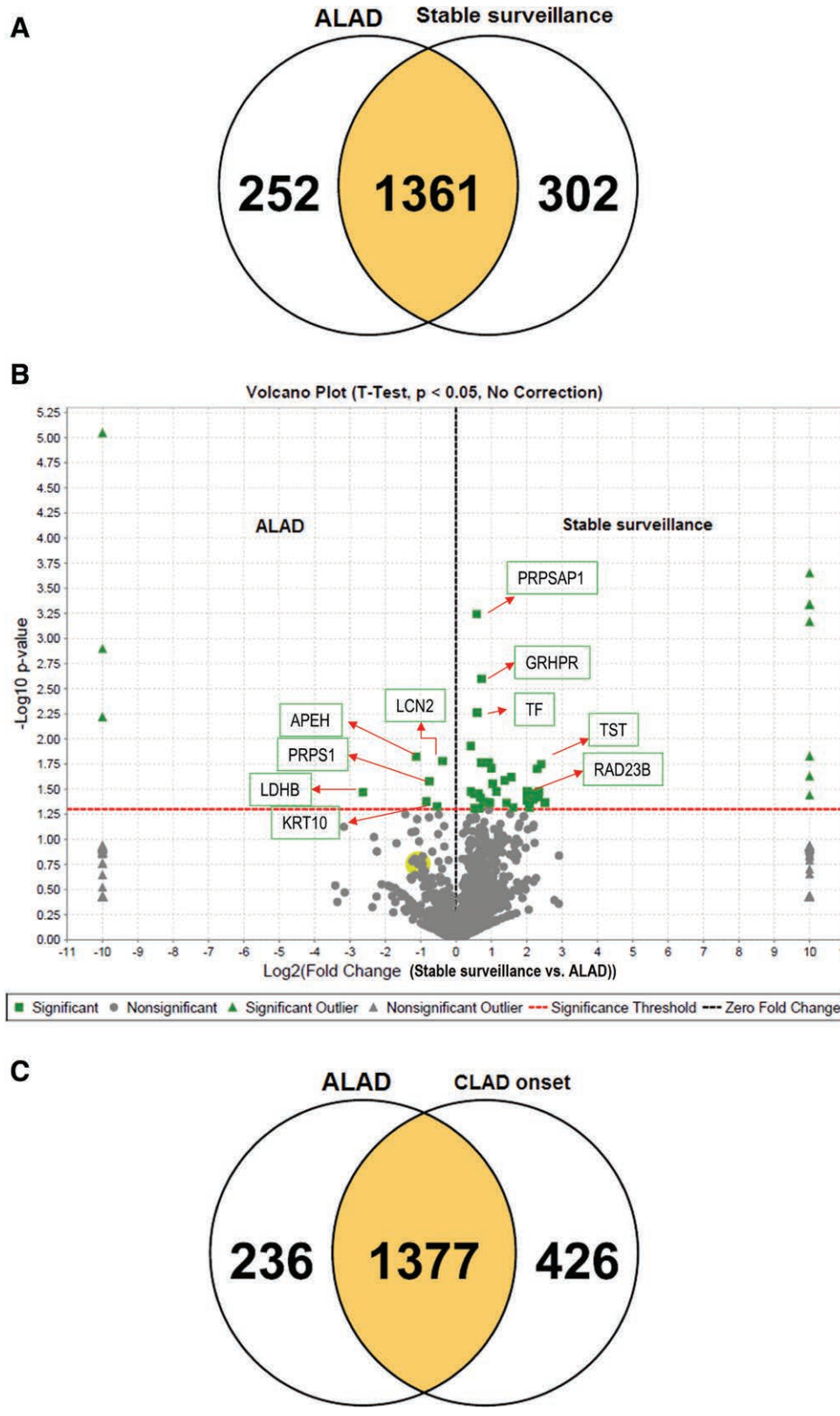

FIGURE 5. Proteomic homology and Volcano plot of DEPs between patients with and without a diagnosis of CLAD. A, Venn diagram showing a high overlap (71.07%) of expressed proteins between the time points of ALAD and stable surveillance. B, Volcano plot of DEPs between ALAD and stable surveillance showed a mild difference. C, The protein homology between ALAD and CLAD onset was 67.53%. E, Venn diagram showing a mild overlap (57.37%) of expressed proteins between the time points of stable surveillance in CLAD and non-CLAD groups. F, Volcano plot of DEPs between the time points of stable surveillance in CLAD and non-CLAD groups showed a significant difference. Volcano plot depicts the log2 fold change (x-axis) vs -log10 Q value (y-axis, representing the probability that the protein is differentially expressed). $P < 0.05$ and fold change ≥1.25 were set as the significant threshold (red line) for differential expression. Dots in green denote significantly upregulated proteins which passed the screening threshold. Black dots present non-significantly DEPs. D, Volcano plot of DEPs between ALAD and CLAD onset showed a significant difference. ALAD, acute lung allograft dysfunction; CLAD, chronic lung allograft rejection; DEPs, differentially expressed proteins.

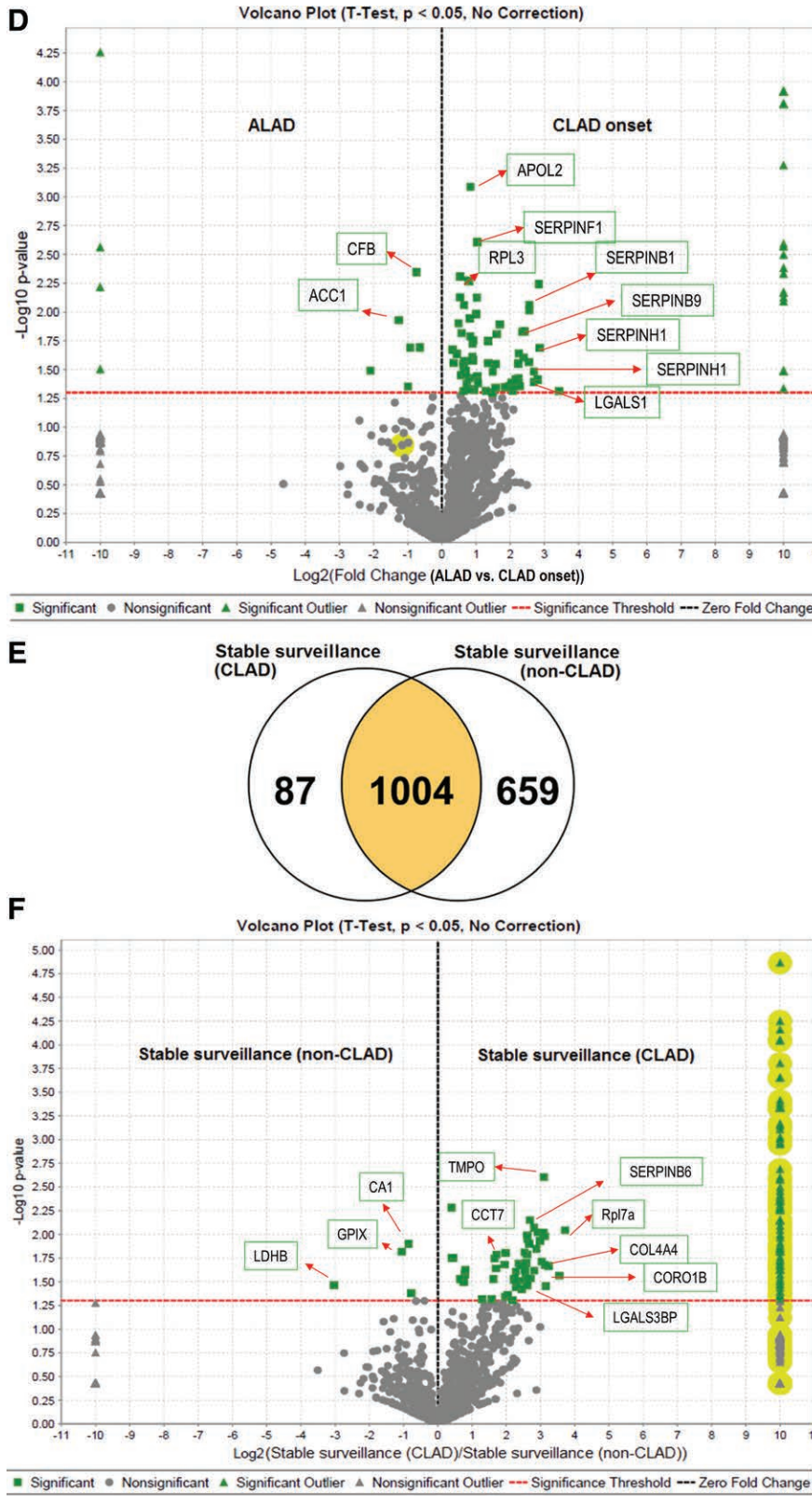

FIGURE 5. Continued

immunohistochemistry staining validated upregulation of SerpinB1, SerpinH1, Cofilin 1, and Coronin1B in TBBx of all cases at timepoints of CLAD onset and explant pathology, and also exhibited a tendency toward higher expression of these proteins, obtained from stable surveillance sampling, to CLAD onset and explant pathology compared with non-CLAD patients. This indicates a possible role of these proteins in CLAD development.

TABLE 3.

Top 60 upregulated proteins in in CLAD onset TBBx compared with ALAD TBBx

Protein	Description	Fold change	*P*
APOL2	Apolipoprotein L2	11	0.049
QDPR	Dihydropteridine reductase	7.3	0.02
NAGK	N-acetyl-D-glucosamine kinase	7.1	0.005
SNRPA	U1 small nuclear ribonucleoprotein A	7.0	0.039
SRP14	Signal recognition particle 14 kDa protein	6.5	0.033
MAN2B1	Lysosomal alpha-mannosidase	6.5	0.041
COTL1	Coactosin-like protein	5.9	0.009
EIF3F	Eukaryotic translation initiation factor 3 subunit F	5.9	0.008
NECAP2	Adaptin ear-binding coat-associated protein 2	5.9	0.027
PRPSAP1	Phosphoribosyl pyrophosphate synthase-associated protein 1	5.4	0.015
LYPLA1	Acyl-protein thioesterase 1	5.4	0.015
PSMB9	Proteasome subunit beta type-9	5.2	0.025
NDUFA9	NADH dehydrogenase [ubiquinone] 1 alpha subcomplex subunit 9	5.1	0.015
DPM1	Dolichol-phosphate mannosyltransferase subunit 1	4.9	0.044
THY1	Thy-1 membrane glycoprotein	4.9	0.044
PDLIM3	PDZ and LIM domain protein 3	4.9	0.044
ATP5MG	ATP synthase subunit g, mitochondrial	4.8	0.023
NDUFA13	NADH dehydrogenase [ubiquinone] 1 alpha subcomplex subunit 13	4.7	0.038
RALB	Ras-related protein Ral-B	4.7	0.028
QKI	Protein quaking	4.7	0.028
Otub1	Ubiquitin thioesterase OTUB1	4.7	0.028
Rab6a	Ras-related protein Rab-6A	4.5	0.038
RPL27	60S ribosomal protein L27	4.3	0.041
TOR1AIP1	Torsin-1A-interacting protein 1	4.2	0.048
STING1	Stimulator of interferon genes protein	4.1	0.041
NPEPPS	Puromycin-sensitive aminopeptidase	3.9	0.044
RPL3	60S ribosomal protein L3	3.6	0.045
ACP1	Low molecular weight phosphotyrosine protein phosphatase	3.2	0.013
GSTK1	Glutathione S-transferase kappa 1	3.0	0.028
SAR1A	GTP-binding protein SAR1a	3.0	0.045
PGAM1	Phosphoglycerate mutase 1	3.0	0.016
LMAN2	Vesicular integral-membrane protein VIP36	2.8	0.033
CTSZ	Cathepsin Z	2.8	0.05
SERPINF1	Pigment epithelium-derived factor	2.5	0.039
RPL10	60S ribosomal protein L10	2.5	0.018
AKR1A1	Aldo-keto reductase family 1 member A1	2.5	0.028
RPS8	40S ribosomal protein S8	2.5	0.048
SERPINB1	Leukocyte elastase inhibitor	2.4	0.028
SEPTIN9	Septin-9	2.3	0.018
DEFA1	Neutrophil defensin 1	2.1	0.036
IGHM	Immunoglobulin heavy constant mu	2.1	0.042
SERPINB9	Serpin B9	2.1	0.031
RPS4X	40S ribosomal protein S4, X isoform	2.0	0.002
UQCRC2	Cytochrome b-c1 complex subunit 2, mitochondrial	2.0	0.01
HSD17B10	3-hydroxyacyl-CoA dehydrogenase type-2	2.0	0.007
EMILIN1	EMILIN-1	1.9	0.048
PFN1	Profilin-1	1.9	0.026
RHOA	Transforming protein RhoA	1.9	0.025
SERPINH1	Serpin H1	1.9	0.044
GNAQ	Guanine nucleotide-binding protein G(q) subunit alpha	1.9	0.019
RPS11	40S ribosomal protein S11	1.9	0.018
TPI1	Triosephosphate isomerase	1.8	0.000
NONO	Non-POU domain-containing octamer-binding protein	1.8	0.016
ETFB	Electron transfer flavoprotein subunit beta	1.8	0.047
RPL23	60S ribosomal protein L23	1.8	0.011
RPS10	40S ribosomal protein S10	1.7	0.005
Gnb1	Guanine nucleotide-binding protein G(I)/G(S)/G(T) subunit beta-1	1.7	0.037
MFAP4	Microfibril-associated glycoprotein 4	1.7	0.005
PPIB	Peptidyl-prolyl cis-trans isomerase B	1.7	0.042
LGALS1	Galectin-1	1.6	0.027

ALAD, acute lung allograft dysfunction; CLAD, chronic lung allograft rejection; TBBx, transbronchial biopsy.

TABLE 4.

Top upregulated proteins in surveillance TBBx of CLAD group compared with surveillance TBBx of non-CLAD patients

Protein	Description	Fold change	*P*
SND1	Staphylococcal nuclease domain-containing protein 1	13	0.009
CAPZA2	F-actin-capping protein subunit alpha-2	12	0.027
ACAA2	3-ketoacyl-CoA thiolase, mitochondrial	9.4	0.022
MAPK3	Mitogen-activated protein kinase 3	8.9	0.035
AKAP2	A-kinase anchor protein 2	8.8	0.021
TST	Thiosulfate sulfurtransferase	8.7	0.011
TMPO	Lamina-associated polypeptide 2, isoforms beta/gamma	8.6	0.0025
Nebl	LIM zinc-binding domain-containing Nebulette	8.5	0.0096
POR	NADPH--cytochrome P450 reductase	8.2	0.019
Rpl7a	60S ribosomal protein L7a	8	0.012
STAT3	Signal transducer and activator of transcription 3	7.6	0.0096
SARG	Specifically androgen-regulated gene protein	7.4	0.014
RUVBL2	RuvB-like 2	7.1	0.024
RALA	Ras-related protein Ral-A	7	0.0085
PDHB	Pyruvate dehydrogenase E1 component subunit beta, mitochondrial	6.5	0.0071
SERPINB6	Serpin B6	6.5	0.029
PA2G4	Proliferation-associated protein 2G4	6.4	0.013
HNRNPUL2	Heterogeneous nuclear ribonucleoprotein U-like protein 2	6.1	0.01
ACADVL	Very long-chain specific acyl-CoA dehydrogenase, mitochondrial	6.1	0.011
RPL5	60S ribosomal protein L5	6.1	0.016
LPCAT1	Lysophosphatidylcholine acyltransferase 1	6.1	0.035
TXN	Thioredoxin	6	0.02
COL4A4	Collagen alpha-4(IV) chain	5.9	0.029
GPD2	Glycerol-3-phosphate dehydrogenase, mitochondrial	5.8	0.015
HNRNPH2	Heterogeneous nuclear ribonucleoprotein H2	5.8	0.024
CORO1B	Coronin-1B	5.5	0.031
UQCRFS1	Cytochrome b-c1 complex subunit Rieske, mitochondrial	5.5	0.038
CTNND1	Catenin delta-1	5.4	0.021
RPL24	60S ribosomal protein L24	5.2	0.02
RPL30	60S ribosomal protein L30	4.9	0.025
GOT2	Aspartate aminotransferase, mitochondrial	4.9	0.036
PGRMC2	Membrane-associated progesterone receptor component 2	4.7	0.03
ESAM	Endothelial cell-selective adhesion molecule	4.7	0.03
SCEL	Sciellin	4.7	0.03
LGALS3BP	Galectin-3-binding protein	4.1	0.044
Sec22b	Vesicle-trafficking protein SEC22b	3.9	0.016
GNAQ	Guanine nucleotide-binding protein G(q) subunit alpha	3.9	0.021
FH	Fumarate hydratase, mitochondrial	3.9	0.046
CCT7	T-complex protein 1 subunit eta	3.3	0.016
ALDH1A1	Retinal dehydrogenase 1	3.2	0.018
HSPA9	Stress-70 protein, mitochondrial	3.2	0.023
TNS1	Tensin-1	3.1	0.03
KPNB1	Importin subunit beta-1	3	0.048
CCT8	T-complex protein 1 subunit theta	2.5	0.048
CBR1	Carbonyl reductase [NADPH] 1	1.7	0.024
DHX9	ATP-dependent RNA helicase A	1.7	0.026
ITGB1	Integrin beta-1	1.7	0.032
IGKC	Immunoglobulin kappa light chain	1.6	0.03

CLAD, chronic lung allograft rejection; TBBx, transbronchial biopsy.

The second group of proteins were those that uniquely expressed in TBBx of the most LTx cases at CLAD onset and explant stages. These include HLA-DQB1, JCHAIN, SAP18, FUCA1, MZB1, G3BP2, and BTF3. Because these proteins were not detected in non-CLAD groups, they have the potential to be further considered for distinguishing of CLAD TBBx from non-CLAD samples upon histopathologic examinations by IHC staining. However, a further study with larger sample size is necessary to validate and monitor these proteins in TBBx of CLAD and non-CLAD groups.

Upregulation of MUC1, SERPINE2, collagens, and some inflammatory and fibrosis-related mediators were already reported in transcriptomic and metabolomics studies.[6,14,15] The discovered proteins in this pilot study at different time points from pre-CLAD to explant state are interesting to be

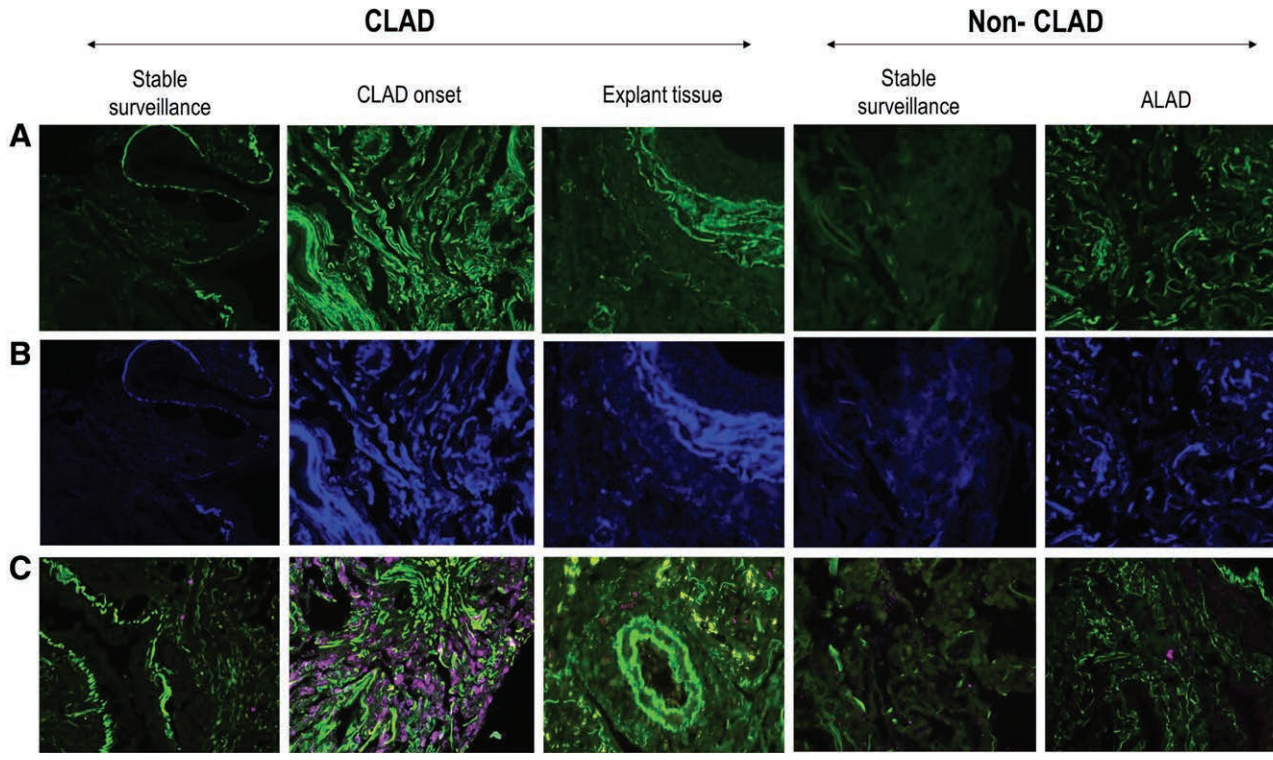

FIGURE 6. Representative immunohistochemistry staining of target proteins in TBBx of LTx patients. IHC staining confirmed the presence and upregulation of SerpinB1 (green color; A), Coronin 1B (blue color; B), and Serpin H1 (purple color; C) and Cofilin 1 (Green color) in TBBx of CLAD and non-CLAD groups. Staining intensity of Serpin B1, Coronin 1B, Serpin H1, and Cofilin 1 was higher in CLAD onset and explant TBBx compared with non-CLAD cases, whereas the staining intensity in stable surveillance state was mild either in CLAD or non-CLAD cases. Original magnification ×63. CLAD, chronic lung allograft rejection; IHC, immunohistochemistry; LTx, lung transplantation; TBBx, transbronchial biopsies.

considered further for early diagnosis of CLAD and graft rejection. We found a trend toward overexpression of these proteins from stable grafts to CLAD and explant tissues that might be the early indicators for CLAD development and lung allograft rejection in LTx recipients. Our in-depth proteome analysis coupled with advanced bioinformatics platforms revealed upregulation and uniquely expression of a number of proteins in CLAD TBBx compared with non-CLAD cases, indicating CLAD is a complicated process in which a wide range of signaling pathways and proteins are involved together. The identified dysregulated proteins are possibly involved in CLAD through multiple main mechanisms or signaling pathways, including leukocytes migration and activation, inflammation, free radicals production and oxidative stress, myofibroblasts activation, epithelial–mesenchymal transition (EMT), and excessive deposition of extracellular matrix (ECM) (Figure 7). All of these pathways are eventually connected to fibrosis and allograft injury as a key pathological feature of CLAD development (Figure 7). For example, upregulation of proteins such as MIF, LGALS3BP, and Coronin 1 triggers migration of inflammatory cells into the allograft leading to the release of multiple proinflammatory mediators and massive production of ROS, which in turn further activate oxidative stress and apoptotic pathways. Upregulation of proteins, especially Serpins, reflects the accumulation of migrated inflammatory cells into the grafts. ROS generation by leukocytes also activates fibroblasts leading to EMT, excessive ECM deposition and fibrosis as the main histologic characteristic of CLAD. Upregulation of CFL-1 protein might induce transdifferentiation of inflammatory cells into fibroblasts as a main source of ROS and excessive accumulation of ECM. SerpinH1, which stimulates Collagens biosynthesis, might be a direct stimulator for excessive accumulation of ECM and further CLAD risk. Overexpression of Mucins, especially MUC1, MUC5AC and MUC5B, in the TBBx of LTx patients might be directly implicated in the development of fibrosis and CLAD.

SerpinB1 or leukocyte elastase inhibitor is a strong inhibitor of serine proteases such as elastase that are often produced and secreted during the neutrophil degranulation.[16,17] Serine proteases are important mediators of inflammation, fibrosis and lung injury when upregulated. SerpinB1 upregulation in TBBx of patients with CLAD most likely reflects the existence of inflammatory cells and protease activity in lung allografts, and may enhance the risk of lung fibrosis and graft injury. Higher level of SerpinB1 and its positive correlation with elastase activity and neutrophil counts were previously reported in BALF of patients with cystic fibrosis.[17] SerpinH1, also known as heat shock protein 47, is a collagen-specific chaperone that plays an essential role in the processing and secretion of collagens.[18] Interestingly, we observed a significant upregulation of SerpinH1 together with collagens COL15A1 and COL4A4 in the TBBx tissue of patients at CLAD onset. Increased expression of collagens in the TBBx of transplanted lungs may be an early signal of the matrix changes and the progression to terminal CLAD. Because collagens are a main component of ECM deposition and fibrosis development, the upregulation of these proteins in TBBx at CLAD onset, may be also associated with higher degree of allograft fibrogenesis, airway remodeling and injury post-transplantation. Our findings align with Jonigk et al[7] where

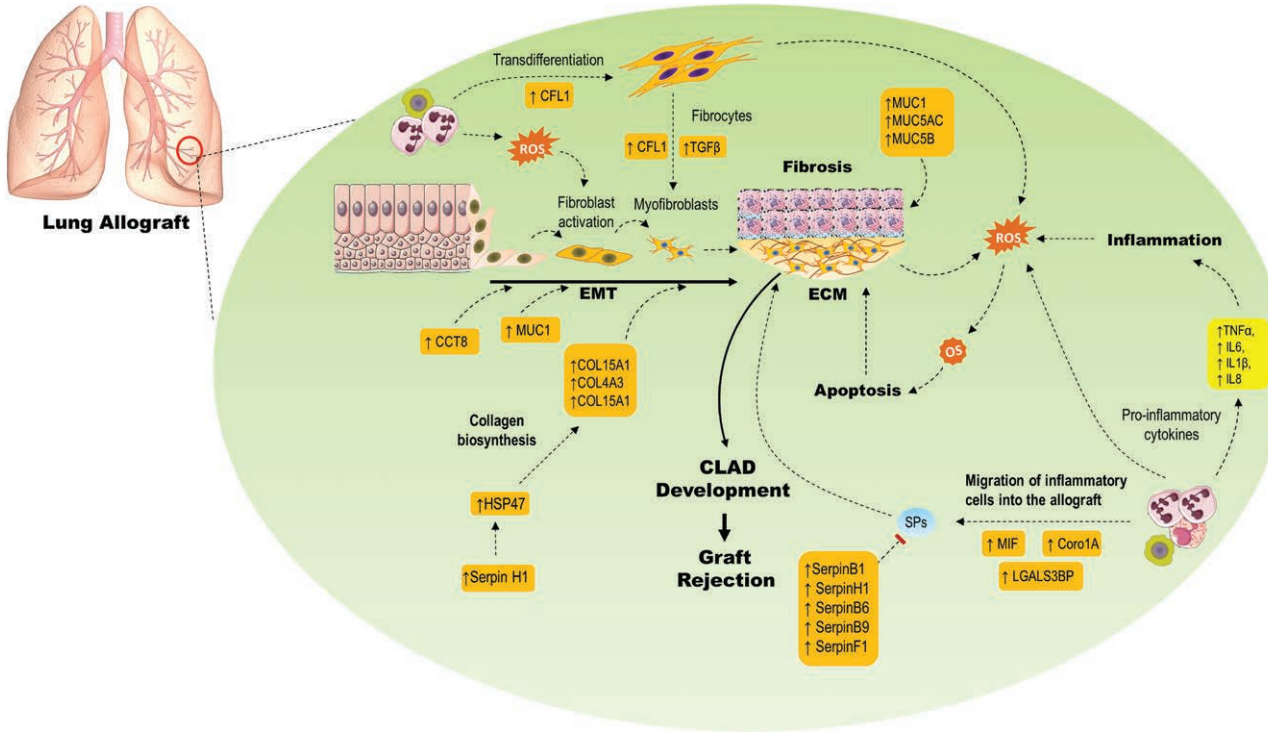

FIGURE 7. Proposed mechanisms of upregulated proteins in CLAD development. Our proteomics analysis revealed upregulation of several proteins (orange color) that are collectively involved in leukocytes migration and activation to the allograft, inflammasome formation, ROS production and oxidative stress, apoptosis, EMT process, excessive ECM deposition, collagen biosynthesis, and fibrosis which in turn enhance the risk of CLAD onset and graft rejection. CLAD, chronic lung allograft rejection; ECM, extracellular matrix; EMT, epithelial–mesenchymal transition; EOS, eosinophilia; ROS, reactive oxygen species.

increased expression of fibrosis-associated genes was found in TBBs from patients with CLAD. Razzaque et al[19] found overexpression of SerpinH1 and accumulation of collagens in fibrotic lung sections. Others have identified an increased number of SerpinH1-positive myofibroblasts in lung biopsies of patients with pulmonary fibrosis.[20] We also found upregulation of other Serpins such as SerpinB6, SerpinB9, and SerpinF1 in TBBx of patients with CLAD compared with non-CLAD patients. A recent Transcriptomic study reported increased expression of SerpinE2 in the TBBx of patients with CLAD.[6] Although the exact function of these inhibitors within the airways of patients with CLAD is unclear, it appears that Serpins are produced in response to elevated proteases activity and inflammation, which may indicate that they are expressed to help suppress the inflammatory response and lung injury.[21] The CLAD development and allograft rejection may be linked to excessive peptidase activity. Therefore, it is not surprising that Serpins can be considered as valuable clinical biomarkers of allograft dysfunction and therapeutically applied to restore normal function of lungs in LTx patients. We propose that Serpins, especially SerpinsB1 and SerpinH1, require consideration and validation as tissue biomarkers for CLAD and allograft dysfunction. They may also represent a novel therapeutic target in LTx patients. To support it, some studies used archetypical Serpin, recombinant α-1-antitrypsin, for treatment of pulmonary diseases such as cystic fibrosis and found some improvements.[22,23] In another study, Bédard et al[24] found that peritransplant SerpinsB1 administration decreased early injury and allowed reduced chronic rejection and interstitial fibrosis in a rat renal model.

Mucin1 (MUC1) is another interesting protein that was significantly upregulated in the tissue of all CLAD cases at the time of CLAD onset. MUC1, also known as KL-6, is a key protein involved in EMT with pro-proliferative and antiapoptotic activities on fibroblasts. EMT, a fibroproliferative process caused by fibroblasts activation and massive release of collagens, is the main trigger of CLAD.[25,26] It may play a pathological role in CLAD development as well as fibrosing lung diseases.[27] Although information on KL-6 in the LTx recipients is scarce, studies have shown increased level of KL-6 in serum and BALF of patients with CLAD.[28,29] Levy et al[15] found increased levels of MUC1, MUC16, MUC5B, and M30 in BALF of patients with CLAD compared with controls. Importantly, higher Mucin concentrations were closely related to poor allograft survival after CLAD onset. In another study, Bessa et al[30] reported that serum MUC1 level could be considered a diagnostic indicator of CLAD development with 86% sensitivity and 78% specificity. Therefore, MUC1 may be a potential biomarker for differentiating the development of CLAD after episodes of ALAD.

We also observed overexpression of CFL-1 and Coronin1B proteins in TBBx of patients with CLAD. CFL-1, a part of the actin depolymerizing factor/cofilin family, is a major mediator for lung fibrogenesis. It induces EMT and ECM formation. Upregulation of CFL-1 in the tissue of LTx patients indicates graft susceptibility towards fibrosis development and may indicate an increased CLAD risk. Recent studies have illustrated that CFL-1 upregulation not only induces the differentiation of fibrocytes from peripheral blood mononuclear cells but also promotes EMT that is associated with ECM

formation and subsequently tissue fibrosis.[31,32] Coronin1 was also upregulated in TBBx of CLAD groups. Coro1 plays a role in the functionality of natural killer cells and neutrophils.[33,34] Recent evidence has demonstrated that Coro1 regulates naive T cells, and its deficiency or deletion in mice model results in tolerance toward allografts.[34] Thus, the predominant expression of Coronin1 in tissue of patients with CLAD in the current study represents a potential mechanism for allograft injury in these patients. Whether therapeutic targeting of Coronin1 may allow improve allograft function and recovery requires further attention. Therefore, these data highlight that multiple signaling pathways and proteins are involved in CLAD pathophysiology. Clarifying of which proteins are directly involved in CLAD development need further extensive in vivo and in vitro studies coupled with advanced technologies such as genomic knockout study by CRISPR/Cas9. Furthermore, further studies are necessary to monitor the expression of each of these proteins in a larger group of patients with different phenotypes (eg, CLAD, Chronic obstructive pulmonary disease, IPF) to validate their specificity and clinical application for early diagnosis of CLAD. Our study opened an opportunity for further studies to monitor these proteins and consider their diagnostic value for identification of patients at higher risk of CLAD.

This study has limitations that merit discussion. First, the sample size was limited, which has affected the statistical power and our ability to detect significant differences in expression patterns of some proteins. Furthermore, we used FFPE specimens, where fixation and embedding of samples may have affected the quality of extracted proteins, leading to inaccurate results. This study had a disproportion of women compared with men in the CLAD group that might affect the clinical LTx and proteomics outcomes between CLAD and non-CLAD groups. The median time to ALAD in the CLAD group (58 mo) was significantly higher than non-CLAD patients (12 mo) that might affect the proteomics signature; however, we performed intragroup proteome analysis to decrease the bias. Since non-CLAD cases were still stable even at 58 mo post-LTx, we did not collect more TBBx at that timepoint. Additionally, the median age of LTx patients in this study was significantly inferior the data reported from the International Thoracic Organ Transplant Registry.[35] Because the age is relevant in several biological processes associated with CLAD and may significantly impact the proteomic profile, our results may be not fully representative of the general LTx populations. Nevertheless, there was a balance in the median age between the 2 groups of patients that reduces the bias in proteomics signature. We believe that the in-depth data analysis in our small longitudinal study provides invaluable insight to direct future work on a larger scale. Further studies with a larger number of fresh biopsy specimens are needed to validate our results. We also recommend measuring the level of these candidate proteins in blood and BALF as a potential noninvasive biomarker for CLAD.

CONCLUSION

This study identifies and validates unique tissue proteins, including SerpinB1, SerpinH1, Cofilin 1, MUC1, COL15A1, COL4A4, Coronin1B, HLA-DQB1, JCHAIN, SAP18, FUCA1, MZB1, G3BP2, and BTF3 that appear to be linked to the development of CLAD. These proteins may represent potential tissue biomarkers for the differentiation of LTx patients at elevated risk of CLAD, especially following episodes of ALAD. Larger studies analyzing these proteins in blood and BALF are essential in defining the role they may play as a noninvasive biomarkers for CLAD.

ACKNOWLEDGMENTS

The authors warmly thank Alexandra and Loyd Martin family for the generous financial support. The authors would also like to acknowledge staff at Lung Transplant Department and SydPath at St. Vincent's Hospital for samples collection and pathological examination; Garvan Institute of Medical Research, Bioanalytical Mass Spectrometry Facility at UNSW, and Centenary Institute at the University of Sydney for technical supports.

REFERENCES

1. Chambers DC, Cherikh WS, Goldfarb SB, et al; International Society for Heart and Lung Transplantation. The international thoracic organ transplant registry of the international society for heart and lung transplantation: thirty-fifth adult lung and heart-lung transplant report-2018; focus theme: multiorgan transplantation. *J Heart Lung Transplant*. 2018;37:1169–1183.
2. Verleden GM, Glanville AR, Lease ED, et al. Chronic lung allograft dysfunction: definition, diagnostic criteria, and approaches to treatment—a consensus report from the Pulmonary Council of the ISHLT. *J Heart Lung Transplant*. 2019;38:493–503.
3. Van Herck A, Verleden SE, Sacreas A, et al. Validation of a post-transplant chronic lung allograft dysfunction classification system. *J Heart Lung Transplant*. 2019;38:166–173.
4. Yoshiyasu N, Sato M. Chronic lung allograft dysfunction post-lung transplantation: The era of bronchiolitis obliterans syndrome and restrictive allograft syndrome. *World J Transplant*. 2020;10:104–116.
5. Verleden SE, Hendriks JMH, Lauwers P, et al. Biomarkers for chronic lung allograft dysfunction: ready for prime time? *Transplantation*. 2023;107:341–350.
6. Parkes MD, Halloran K, Hirji A, et al. Transcripts associated with chronic lung allograft dysfunction in transbronchial biopsies of lung transplants. *Am J Transplant*. 2022;22:1054–1072.
7. Jonigk D, Izykowski N, Rische J, et al. Molecular profiling in lung biopsies of human pulmonary allografts to predict chronic lung allograft dysfunction. *Am J Pathol*. 2015;185:3178–3188.
8. Verleden SE, Verleden GM. Novel biomarkers of chronic lung allograft dysfunction: is there anything reliable? *Curr Opin Organ Transplant*. 2022;27:1–6.
9. Tissot A, Durand E, Goronflot T, et al; COLT Consortium. Blood MMP-9 measured at 2 years after lung transplantation as a prognostic biomarker of chronic lung allograft dysfunction. *Respir Res*. 2024;25:88.
10. Peris MA, Mendoza-Valderrey A, Ruiz V, et al. Prediction of chronic lung allograft dysfunction by serum KL-6 levels. *Eur Respir J*. 2023;62(Suppl 67):OA4344.
11. Tissot A, Danger R, Claustre J, et al. Early identification of chronic lung allograft dysfunction: the need of biomarkers. *Front Immunol*. 2019;10:1681.
12. Diel R, Simon S, Gottlieb J. Chronic lung allograft dysfunction is associated with significant disability after lung transplantation-a burden of disease analysis in 1025 cases. *Adv Respir Med*. 2023;91:432–444.
13. Todd JL. Putting the 2019 CLAD consensus definitions to the test: two steps forward, one step back? *J Heart Lung Transplant*. 2020;39:771–773.
14. Mohanty RP, Moghbeli K, Singer JP, et al. Small airway brush gene expression predicts chronic lung allograft dysfunction and mortality. *J Heart Lung Transplant*. 2024;43:1820–1832.
15. Levy L, Moshkelgosha S, Huszti E, et al. Pulmonary epithelial markers in phenotypes of chronic lung allograft dysfunction. *J Heart Lung Transplant*. 2023;42:1152–1160.
16. Cooley J, Takayama TK, Shapiro SD, et al. The serpin MNEI inhibits elastase-like and chymotrypsin-like serine proteases through efficient reactions at two active sites. *Biochemistry*. 2001;40:15762–15770.

17. Cooley J, Sontag MK, Accurso FJ, et al. SerpinB1 in cystic fibrosis airway fluids: quantity, molecular form and mechanism of elastase inhibition. *Eur Respir J*. 2011;37:1083–1090.
18. Sakamoto N, Okuno D, Tokito T, et al. HSP47: a therapeutic target in pulmonary fibrosis. *Biomedicines*. 2023;11:2387.
19. Razzaque MS, Nazneen A, Taguchi T. Immunolocalization of collagen and collagen-binding heat shock protein 47 in fibrotic lung diseases. *Mod Pathol*. 1998;11:1183–1188.
20. Iwashita T, Kadota J, Naito S, et al. Involvement of collagen-binding heat shock protein 47 and procollagen type I synthesis in idiopathic pulmonary fibrosis: contribution of type II pneumocytes to fibrosis. *Hum Pathol*. 2000;31:1498–1505.
21. Kelly-Robinson GA, Reihill JA, Lundy FT, et al. The serpin superfamily and their role in the regulation and dysfunction of serine protease activity in COPD and other chronic lung diseases. *Int J Mol Sci*. 2021;22:6351.
22. Gaggar A, Chen J, Chmiel JF, et al. Inhaled alpha1-proteinase inhibitor therapy in patients with cystic fibrosis. *J Cyst Fibros*. 2016;15:227–233.
23. Martin SL, Downey D, Bilton D, et al; Recombinant AAT CF Study Team. Safety and efficacy of recombinant alpha(1)-antitrypsin therapy in cystic fibrosis. *Pediatr Pulmonol*. 2006;41:177–183.
24. Bédard ELR, Jiang J, Arp J, et al. Prevention of chronic renal allograft rejection by SERP-1 protein. *Transplantation*. 2006;81:908–914.
25. Müller C, Rosmark O, Åhrman E, et al. Protein signatures of remodeled airways in transplanted lungs with bronchiolitis obliterans syndrome obtained using laser-capture microdissection. *Am J Pathol*. 2021;191:1398–1411.
26. Armati M, Cattelan S, Guerrieri M, et al; Tuscany Transplant Group. Collagen type IV Alpha 5 chain in bronchiolitis obliterans syndrome after lung transplant: the first evidence. *Lung*. 2023;201:363–369.
27. Ohshimo S, Yokoyama A, Hattori N, et al. KL-6, a human MUC1 mucin, promotes proliferation and survival of lung fibroblasts. *Biochem Biophys Res Commun*. 2005;338:1845–1852.
28. Walter JN, Fan LL, Bag R, et al. Serum KL-6 as a marker for bronchiolitis obliterans syndrome after lung transplantation. *Transplantation*. 2006;82:709–711.
29. Berastegui C, Gómez-Ollés S, Mendoza-Valderrey A, et al. Use of serum KL-6 level for detecting patients with restrictive allograft syndrome after lung transplantation. *PLoS One*. 2020;15:e0226488.
30. Bessa V, Bonella F, Ohshimo S, et al. Changes in serum KL-6 levels are associated with the development of chronic lung allograft dysfunction in lung transplant recipients. *Transpl Immunol*. 2019;52:40–44.
31. Guo W, Guo T, Zhou Q, et al. Cofilin-1 promotes fibrocyte differentiation and contributes to pulmonary fibrosis. *Biochem Biophys Res Commun*. 2021;565:43–49.
32. Hassani E, Shekari Khaniani M, Saffari M, et al. Differential expression pattern of epithelial mesenchymal transition gens: AXL, GAS6, Claudin-1, and Cofilin-1, in different stages of epithelial ovarian cancer. *Iran J Public Health*. 2019;48:1723–1731.
33. Tchang VSY, Stiess M, Siegmund K, et al. Role for coronin 1 in mouse NK cell function. *Immunobiology*. 2017;222:291–300.
34. Jayachandran R, Gumienny A, Bolinger B, et al. Disruption of coronin 1 signaling in T Cells promotes allograft tolerance while maintaining anti-pathogen immunity. *Immunity*. 2019;50:152–165.e8.
35. Chambers DC, Perch M, Zuckermann A, et al; International Society for Heart and Lung Transplantation. The international thoracic organ transplant registry of the international society for heart and lung transplantation: thirty-eighth adult lung transplantation report-2021; focus on recipient characteristics. *J Heart Lung Transplant*. 2021;40:1060–1072.